

Crossover from a fission-evaporation scenario towards multifragmentation in spallation reactions

P. Napolitani ^{a,b}

^aGANIL (DSM-CEA/IN2P3-CNRS), Blvd. H. Becquerel, 14076 Caen, France

^bLPC (IN2P3-CNRS), 14076 Caen, France

Abstract

Mostly for the purpose of applications for the energy and the environment and for the design of sources of neutrons or exotic nuclides, intense research has been dedicated to spallation, induced by protons or light projectiles at incident energies of around 1 GeV. In this energy range, while multifragmentation has still a minor share in the total reaction cross section, it was observed to have, together with fission, a prominent role in the production and the kinematics of intermediate-mass fragments, so as to condition the whole production of light and heavy nuclides. The experimental observables we dispose of attribute rather elusive properties to the intermediate-mass fragments and do not allow to classify them within one exclusive picture which is either multifragmentation or fission. Indeed, these two decay mechanisms, driven by different kinds of instabilities, exhibit behaviours which are closely comparable. High-resolution measurements of the reaction kinematics trace the way for probing finer features of the reaction kinematics.

Conference proceedings: International Meeting "Selected topics on nuclear methods for non-nuclear applications", September 27-30, 2006, Varna

1 Introduction

Sixty years passed from Serber's early description [1] of high-energy nuclear reactions induced by nucleons and light nuclei. In their main outline, such reactions are described as the exciting of an atomic nucleus, followed by a decay process in several nuclides, clusters, protons and neutrons [2]. Several different nuclear systems have been explored with beams of various incident energies, at different facilities and with different experimental techniques. Numerous experimental results and various observables on the production of residues, on

the kinematics of the emission of ejectiles and fragments, and on the correlations inspired and constrained the physical models.

At incident energies of few hundred MeV per nucleon, an excited and fully equilibrated complex, named compound nucleus, is formed and successively de-excites by mainly fission-evaporation decays. When the excitation energy of the hot nucleus exceeds the threshold for emission of particles or clusters (including fission), the system has the possibility to decay by any of the open channels. If the excited system is not too hot, the favoured process is the re-ordering of its configurations: a great number of arrangements are available where all nucleons remain in states below the continuum, occupying excited single-particle levels around the Fermi surface. Rather seldom, compared with this thermal chaotic motion of the system, one nucleon acquires enough energy to pass above the continuum and may eventually leave the nucleus. This picture was extended to include the production of intermediate-mass fragments by cluster decay and oscillations in fission direction as well. In this respect, there would be a gradual transition from very asymmetric to symmetric configurations in the binary split of the decaying compound nucleus, so that evaporation of nucleons and light nuclei on the one hand and symmetric fission on the other hand are just the opposite extremes of the manifestation of the same process. This generalisation, introduced by Moretto [3,4], allows to name fission in a generalised sense all (binary) decays of a compound nucleus. Since this decay is a rare process, one evaporation event, or fission event, proceeds after the other, sequentially.

At incident energies of some GeV per nucleon, a very highly excited composite nuclear system is formed; it undergoes a violent de-excitation processes, named multifragmentation, which manifests by the production of several massive fragments filling broad kinetic-energy spectra. General reviews on this process can be found in refs. [5,6]; a more specific review treating multifragmentation induced with high-energy proton beams can be found in ref. [7]. The amount of experimental evidence suggests to describe the de-excitation as a simultaneous disassembling of the hot nucleus in several constituents. From the experimental observation of angle correlations between fragments, it was found that the emission of two fragments with small relative angles is highly improbable. Such a dependence on relative emission angles is on the contrary absent for the ejectiles of a sequential evaporation process [8]. The disintegration is so rapid to be considered “simultaneous”, in the sense that it evolves in so short a time interval (10^{-22} - 10^{-21} s) that fragments can still exchange interactions while they are accelerated in their mutual Coulomb field. On the other hand, the process is expected to be still sufficiently “slow” to exceed the relaxation time of the strong interactions and, for this reason, the system is assumed to be thermalised before it disintegrates. Within a thermodynamical picture, multifragmentation is a phenomenon related to the equation of state of nuclear matter [9,10]; with a certain resemblance with Van-der-Waals fluid,

hot bulk matter would enter the liquid-gas coexistence region of the phase diagram and separate in the corresponding coexisting liquid and gas phases (see refs. [12,11] for review), driven by a rapid amplification of spinodal instabilities [13]. According to the same picture, when the composite system reaches the conditions for disintegrating, it should be diluted to some fractions of the nuclear saturation density. These low densities are reached as a result of a dynamical process of expansion, which is expected to explain the high velocity of the fragments observed experimentally. There are however also alternative mechanisms proposed to explain the experimental features of the multifragmentation process which are close to the fully equilibrated compound-nucleus decay [14,15].

In recent years, mostly for the purpose of energetic and environmental applications, as well as for the production of beams of neutrons or exotic nuclides in accelerator facilities, increasing interest is devoted to spallation reactions induced by protons or deuterons at incident energies close to 1 GeV. At this energy, the reaction is situated somehow in between the two scenarios described above and is particularly interesting for studying the transition from fission to multifragmentation. The physics underlying the spallation process in this energy range is however rather uncontrolled. From the experimental side, the approaches used up to now have always provided a partial survey of all the observables which are necessary to formulate conclusive answers. Inclusive approaches are best suited for the identification of the nuclides, for the measurement of the corresponding production cross sections and kinetic-energy distributions; they however neither provide particle correlations, like the multiplicity of the fragments and particles formed in the reaction, nor angle (or velocity) correlations, necessary to probe the reaction kinematics for each single event. Correlation observables are the specificity of exclusive approaches, based on the employment of multidetectors which, at the moment, are still not able to provide the full isotopic identification up to heavy elements and high-resolution velocity measurements. On the other hand, from the modelling side, several different strategies based either on a generalised fission-evaporation scenario [3,16] or on a statistical description of multifragmentation [17,18,19,20,21,22,23,24] have been able to describe the same experimental data with comparable accuracy.

2 Residue production in spallation induced by 1 GeV protons

The measurement of the production of spallation residues at relativistic energy has been the purpose of several years of experiments performed at the FRagment Separator [25,26] (GSI, Darmstadt). The reactions were measured in inverse kinematics, by directing heavy-ion beams at various energies on a target of liquid hydrogen or deuterium. Fig. 1 presents a survey on the nuclide

production for the spallation reactions induced by protons at 1 GeV which were measured at the FRagment Separator.

For the reaction $^{238}\text{U}_{(1\text{ A GeV})} + p$ [27] the nuclide distribution reflects the interplay of more decay patterns. Quite independently on the entrance channel (and in particular the neutron enrichment of the compound nucleus), evaporation residues [28] populate the neutron-poor side of the nuclide chart around the residue corridor [29], which corresponds to the situation where [30]

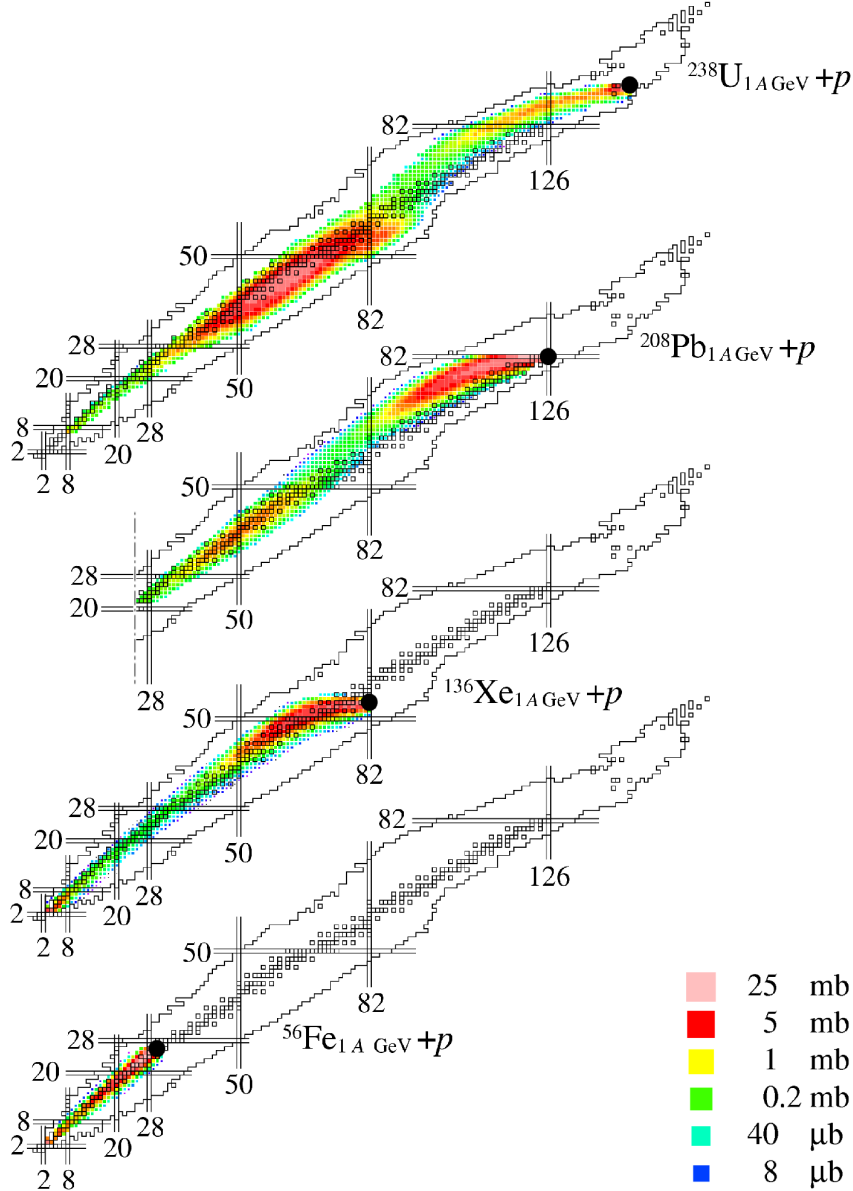


Fig. 1. Experimental survey on the distribution of spallation residues presented in nuclide charts for the systems $^{238}\text{U}_{(1\text{ A GeV})} + p$ [27,28,31,32,33], $^{208}\text{Pb}_{(1\text{ A GeV})} + p$ [34,35], $^{136}\text{Xe}_{(1\text{ A GeV})} + p$ [40], and $^{56}\text{Fe}_{(1\text{ A GeV})} + p$ [37,36]. Filled circles indicate the projectiles (in inverse kinematics).

$dN/dZ = \langle \Gamma_N/\Gamma_Z \rangle$, where Γ_Z and Γ_N are the proton- and neutron-emission width, respectively. This is for instance the reason why neutron-rich nuclei are favoured materials for neutron sources. In the centre of the nuclide distribution an imposing high-energy fission hump emerges between two shoulders generated by low-energy fission channels [31], which are exotic and asymmetric. Other asymmetric fission channels are determined by high-energy fission, as an extension of the central hump; they overlap with the evaporation production on one side [32] and extend to the intermediate-mass fragments [33] on the opposite side.

While uranium is an attractive material for the production of exotic nuclei by low-energy fission, lead is preferred as a neutron source because, as the measurement of $^{208}\text{Pb}_{(1\text{ A GeV})} + p$ reveals [34,35], fission is much reduced with respect to evaporation channels.

Iron was measured because it is a structural material in nuclear installations. From a phenomenology point of view, the results on the reaction $^{56}\text{Fe}_{(1\text{ A GeV})} + p$ [37,36] brought the attention to light systems, below the Businaro-Gallone point [38,39]. At variance with heavy systems, the fission potential becomes convex and fission channels are asymmetric. Moreover, the excitation energy is larger in lighter systems when reactions are compared at the same incident energy. As a result of reaction models [37], for small impact parameters the excitation energy of the composite system generated in the reaction $^{56}\text{Fe}_{(1\text{ A GeV})} + p$ is found to even exceed 3 MeV per nucleon; around this value multifragmentation is expected to set in. For the production of intermediate-mass fragments, this process sums up to the asymmetric fission channels.

The measurement of $^{136}\text{Xe}_{(1\text{ A GeV})} + p$ was performed on purpose to analyse the intermediate-mass-fragment production and its influence on the overall decay mechanism. In this respect, ^{136}Xe offers an optimum point of observation: symmetric fission, which in heavier systems hides the intermediate-mass-fragment production, is suppressed because the system is slightly below the Businaro-Gallone point; then, below the Businaro-Gallone point, ^{136}Xe is the stable nuclide with the largest neutron excess $N - Z$, and it approaches the neutron enrichment N/Z of ^{208}Pb , so that a comparison can be made between the two systems; and finally, the system $^{136}\text{Xe}_{(1\text{ A GeV})} + p$ is excited right enough to still allow for some oscillations towards multifragmentation. The results on the nuclide production [40] illustrate that, besides a close similarity with the system $^{208}\text{Pb}_{(1\text{ A GeV})} + p$ for the evaporation features, beyond a mass loss of around $\Delta A = 70$, the ridge of the residue production abandons the neutron-poor side of the nuclide chart around $Z = 40$ and migrates progressively towards the neutron-rich side for lighter residues. The lightest residues even populate the neutron rich side of the nuclide chart with respect to the valley of stability.

It may be remarked that both asymmetric fission channels and multifragmen-

tation of a neutron-rich composite system produce residues with high neutron excess in the average; the successive evaporation of residues, which is expected due to the high mean excitation energy of the system, contributes to further dissipate the traces of the initial stage of the decay process [41]. Qualitatively, both the two mechanisms also result in a similar U-shape of the mass distribution of residues, with decreasing depth of the hollow for increasing mean excitation energy of the system. For this reason, the residue production alone is a rather elusive observable and it could be reproduced with comparable quality both on the basis of multifragmentation processes and asymmetric fission.

3 Kinematics

More robust observables for the reaction mechanism are those related to the Coulomb field experienced by the fragments. In exclusive experiments, these are angle correlations among fragments, which reflect the role of the Coulomb field in each event; such experimental strategy, based on multidetectors and largely used for ion-ion collisions or for multifragmentation induced by high-energy protons, was unfortunately not employed in the study of spallation in the incident-energy range of around 1 GeV. In inclusive experiments, the observables probing the Coulomb field are the mean quantities related to the momentum distribution of fragments. Evidently, inclusive observables mixes up the contributions of all processes responsible for the formation of one given fragment; therefore, the identification of the reaction process can not be imposed from a selection of separate observables (like the fragment multiplicity or the transferred energy of light charged particle in exclusive experiments [42]), but it should be extracted by the momentum distribution itself. Up to a certain extent, this is possible with magnetic spectrometers operated in inverse kinematics, as in the case of the experiments discussed in section 2, where the high-resolution momentum distributions could be deduced from the measurement of the magnetic rigidity $B\rho$, as precise as $5 \cdot 10^{-4}$ (FWHM) for individual reaction products.

A dedicated analysis procedure (refs. [37,40] for detailed discussion) was applied to reconstruct invariant cross sections from the inclusive measurement of the momentum distribution at the FRagment Separator. An overview of the result is shown in fig. 2 for some light residues of the reaction $^{136}\text{Xe}_{(1\text{ A GeV})} + p$. More details of this observable are shown for the nuclide ^{20}F : in the insert (a), a planar cut along the beam axis of the full velocity distribution in the projectile frame is shown in the $v_{\perp} \times v_{\parallel}$ space (v_{\perp} and v_{\parallel} are respectively the perpendicular and parallel velocity components of the fragment ^{20}F in the beam frame), as reconstructed from the measured momentum distribution; by selecting the velocities aligned along the beam axis, this representation can

be reduced to the distribution of invariant cross section σ_I as a function of v_{\parallel} in the projectile frame, shown in the insert (b). The distribution of invariant cross section σ_I of all the intermediate mass fragments formed in the reaction $^{136}\text{Xe}_{(1\text{ AGeV})} + p$ results from the overlap of two shapes: a component with a convex centre and a component with a concave centre.

A “convex” mode describes two completely different situations. In a first case,

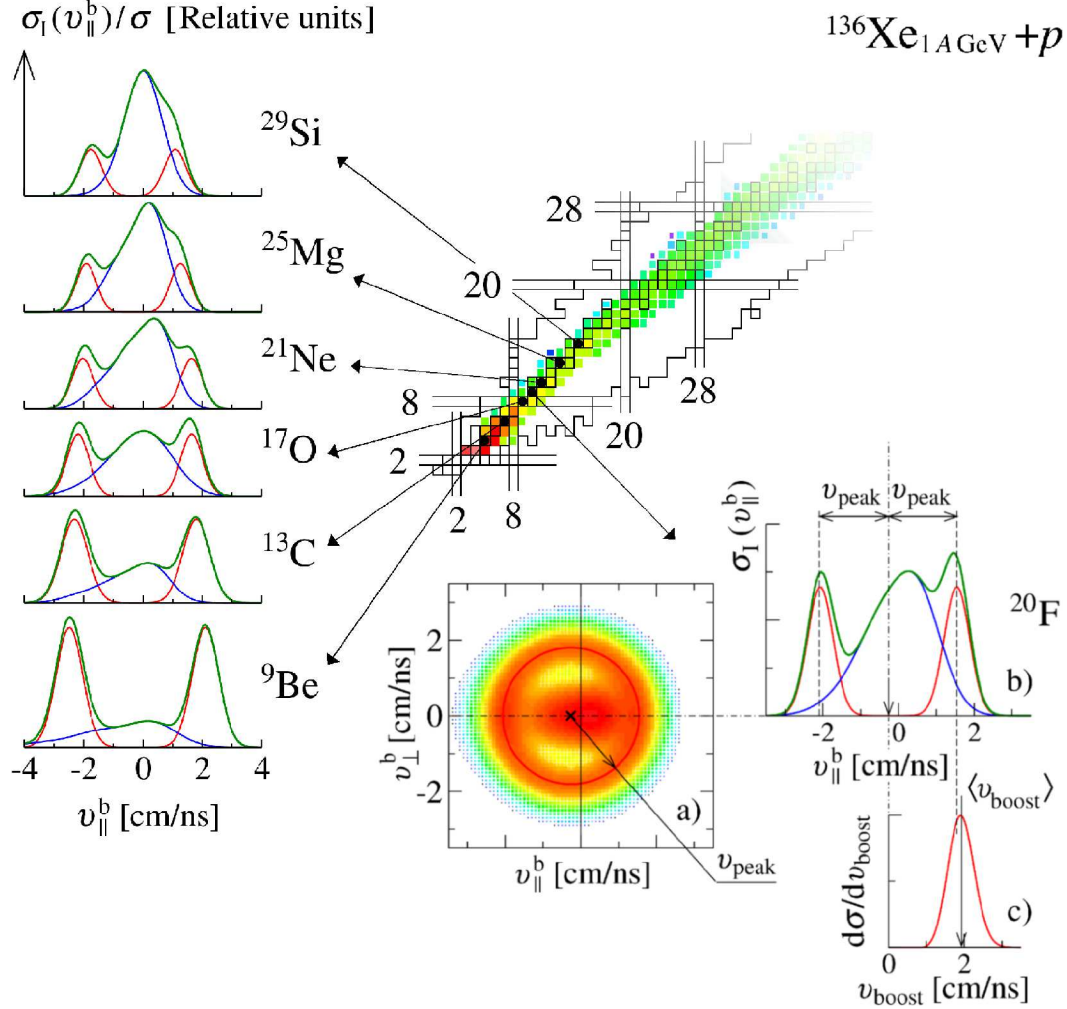


Fig. 2. Distribution of invariant cross section for some intermediate mass fragments produced in the reaction $^{136}\text{Xe}_{(1\text{ AGeV})} + p$ [40]. The corresponding nuclides are indicated on a portion of the fragment distribution, on the nuclide chart. Two kinematical modes, one convex in the centre, the other concave in the centre, are indicated. For the nuclide ^{20}F more details are shown: (a) The planar cut along the beam axis of the reconstructed full distribution $d\sigma/d\mathbf{v}^b$ in the beam frame as a cluster plot. The concave mode is indicated by the corresponding circular ridge of radius v_{peak} . (b) The invariant-cross-section distribution, as for the other nuclides. (c) Reconstructed cross-section distribution for the concave mode as a function of the boost velocity in the source frame v_{boost} . The plot allows to calculate the mean boost $\langle v_{\text{boost}} \rangle$, which differs from v_{peak} .

it describes the velocity distribution of evaporation residues after sequential emission of nucleons and clusters. At these incident energies, the most probable excitation energy is just sufficient for the emission of few nucleons and the probability of higher excitations, connected with longer evaporation paths, can only decrease progressively; this behaviour ensures that the distribution of (heaviest) evaporation residues drops in cross section monotonically when moving away from the projectile and its contribution to the production of intermediate mass fragments is invisible for all the systems described in fig. 1. For these systems, a convex distribution of invariant cross section associated to intermediate mass fragments rather indicates a multifragmentation process; in particular, the convex mode probes the Coulomb field produced by the disassembling of the system in more fragments having a comparable size. The explanation for the asymmetry of this mode, characterised by a long tail in backward direction and a maximum shifted forward, may be searched in possible dynamical effects. It may be interesting to remark that the convex mode, associated to multifragmentation, can not be observed in direct kinematics because a threshold in kinetic energy hides the centre of the distribution of invariant cross section. The “concave mode” reflects a strong Coulomb boost as experienced by fission fragments. When this pattern is associated to intermediate-mass fragments, it may indicate an asymmetric fission process as well as the possible extension of multifragmentation events to very asymmetric partitioning configuration; in this latter case, the kinematics is determined by the repulsion exerted by one very heavy fragment and it should not be disturbed greatly by the presence of more than one light fragment. In conclusion, a concave component in the distribution of invariant cross section of intermediate-mass fragments indicates that the system certainly broke up asymmetrically, but the attribution of the process to fission or multifragmentation stays uncertain on the basis of this inclusive observable.

In fig. 2, the insert (c) represents for the nuclide ^{20}F the convex component alone in polar coordinates in the frame of the corresponding average emitting source. The mean value of this spectrum $\langle v_{\text{boost}} \rangle$ would be consistent with a fission barrier if the process were exclusively reduced to fission. Such test is shown in fig. 3 for some light elements produced in the system $^{136}\text{Xe}_{(1\text{ A GeV})} + p$. The figure compares the measured mean boost $\langle v_{\text{boost}} \rangle$ with the highest expected value, determined by the split of the heaviest possible system, ^{136}Xe . The expected boost is the highest when the fission fragments are considered not deformed and subjected to the fusion potential, as described by the empirical formula of Bass [43,?]. The lowest value is calculated when the fission fragments are considered deformed and joined through a neck according to the liquid-drop picture (scission-point model of Wilkins et al. [45,?]). In between, is situated the value calculated from a systematics of total kinetic energy for light fissioning nuclei [47], further modified in ref. [37] to describe asymmetric splits. The lighter are the elements, the more all the three expectations underpredict the data. This test suggests that the concave mode should be

alimented, in addition to fission, also by multifragmentation channels which could be related to an expansion process and could enhance the mean boost.

Similar experimental observations were collected for the system $^{56}\text{Fe}_{(1\text{ A GeV})} + p$ [37]. In the system $^{238}\text{U}_{(1\text{ A GeV})} + p$, the intermediate-mass fragments were fully described by the concave mode; also in this case, the corresponding mean boost was characterised by very high values [33] so that it is tempting to make a comparison with the lighter systems $^{56}\text{Fe}_{(1\text{ A GeV})} + p$ and $^{136}\text{Xe}_{(1\text{ A GeV})} + p$.

4 Concluding remarks

In conclusion, the coupling of kinematical and production observables is a rather robust approach to study the reaction mechanism in such a complex situation as spallation reactions at incident energies of around 1 GeV. This approach indicated that multifragmentation is a possible decay pattern and determines the kinematics by producing a convex component in the distribution of invariant cross section. More difficult is to define its possible extension to the asymmetric breakups of the system, determined by a concave component in the distribution of invariant cross section. Is the observation of a very high mean boost in the asymmetric splits a signature of dynamical effects, like expansion, which goes mostly in the direction of multifragmentation?

The left panel of fig. 4 shows the mass distribution of the residues of the system

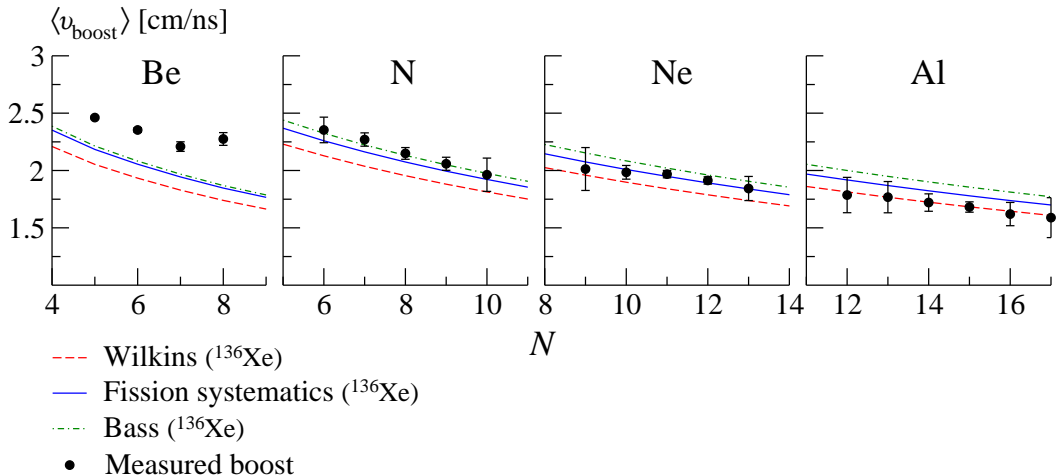


Fig. 3. Evolution of the reconstructed mean boost, deduced for the convex kinetic mode as a function of the neutron number for some light elements in the reaction $^{136}\text{Xe}_{(1\text{ A GeV})} + p$ [40]. The measurement is compared with three expectations for the Coulomb boost in the split of ^{136}Xe , according to the total-kinetic-energy systematics of Tavares and Terranova [47], the scission-point model of Wilkins et al. [45,?] and the nucleus-nucleus fusion model of Bass [43,?].

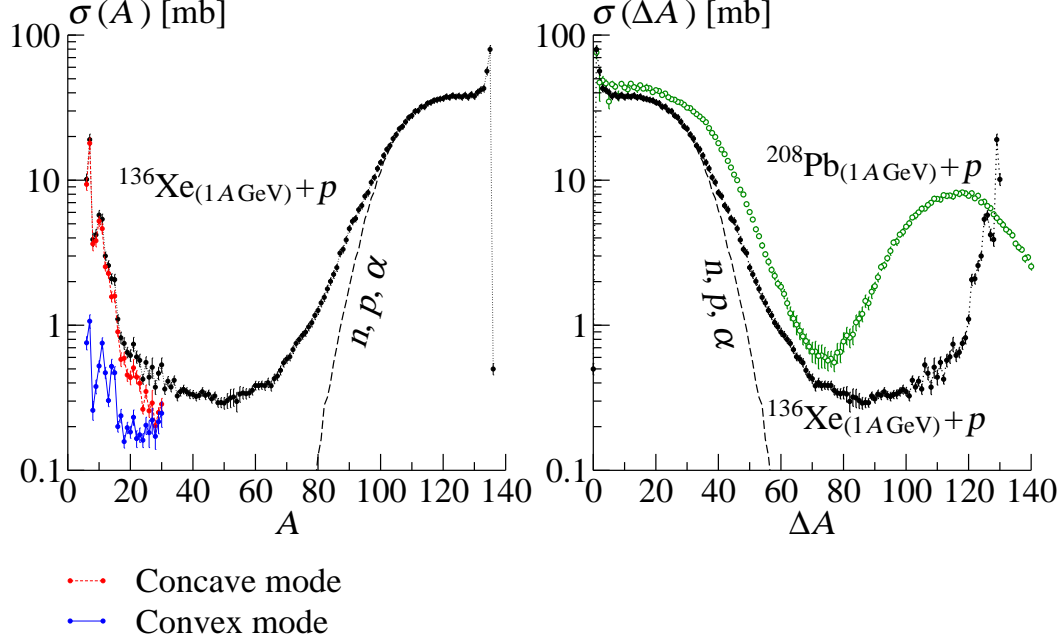


Fig. 4. Left panel. Projections of the residue-production cross sections along the mass number for the system $^{136}\text{Xe}(1\text{A GeV}) + p$ [40]. For intermediate mass fragments the contributions from the two kinematical modes, concave and convex, are indicated. A Weisskopf calculation for the expected contribution of the evaporation of protons, neutrons and alpha particles is shown. Right panel. Mass-loss distribution of production cross sections. The experimental results obtained for the systems $^{136}\text{Xe}(1\text{A GeV}) + p$ [40] and $^{208}\text{Pb}(1\text{A GeV}) + p$ [34] are compared. The same Weisskopf calculation for the system $^{136}\text{Xe}(1\text{A GeV}) + p$ shown in the left panel, is repeated for comparison.

$^{136}\text{Xe}(1\text{A GeV}) + p$. It also shows for the concave and convex kinematical modes the corresponding contribution to the production cross section. The limitations of the experimental approach did not allow to complete the distribution for these two components over the whole mass distribution. However, we can appreciate a rise in cross section of the convex mode up to joining the value of the concave mode. The convex mode is expected to extend further and to be the dominant mode in the region of the hollow of the mass distribution. The concave mode, which gives the highest contribution in the production of the light nuclides, drops steeply in cross section in proximity of the hollow. Since this mode supposes the existence of a heavy partner in a split of mostly binary kind, the corresponding distribution of cross section should also alight the region of heavy masses. The side of the mass spectrum in the region of heavy masses is often taken as a reference for testing the modelling of the initial stage of the reaction process (cascade), due to its sensitivity to the excitation energy introduced in the system during the collision. However, already at incident energies of around 1 GeV, the contribution of the convex mode to the production of heavy masses should greatly modify the slope of the mass distribution for the heavy-fragment side of the hollow, with respect to the

function characterising a more simple mechanism where only protons, neutrons and alpha particles are emitted. Such function, which can be estimated by a Weisskopf calculation, drops to imperceptible cross sections for a mass loss ΔA of less than sixty units and deviates from the experimental distribution already after $\Delta A \approx 40$. The right panel of fig. 4 shows that the cross section evolves with the mass loss in a very similar way for the system $^{136}\text{Xe}_{(1\text{ A GeV})} + p$ and $^{208}\text{Pb}_{(1\text{ A GeV})} + p$ in the region of heavy masses.

This feature reinforces the idea that the concave mode, associated to a fast fission-like process, and observed in the velocity spectra for systems of different size, from $^{56}\text{Fe}_{(1\text{ A GeV})} + p$ to $^{238}\text{U}_{(1\text{ A GeV})} + p$, is a rather general picture in spallation reactions induced by 1 GeV protons. On the other hand, the concave mode, more evidently related to multifragmentation, is a characteristic of more excited system.

The purpose of this report was to outline the main phenomenological features of spallation in the incident-energy range of 1 GeV per nucleon, without discussing any consequence on applications. It however derives naturally that the passage from the phenomenology to the modelling is necessary for application purposes, in order to better describe the overall production of nuclides and the kinematics of light fragments in spallation reactions which are and will be largely employed in energetic and environmental applications.

Acknowledgments

This contribution uses the results of many experiments, performed at the FRagment Separator (GSI, Darmstadt) by the collaboration of the following scientists: P. Armbruster, L. Audouin, A. Bacquias, J. Benlliure, M. Bernas, A. Boudard, E. Casarejos, J. J. Connell, S. Czajkowski, J.-E. Ducret, T. Enqvist, T. Faestermann, B. Fernandez, L. Ferrant, J. S. George, L. Giot, F. Hammache, A. Heinz, K. Helariutta, V. Henzl, D. Henzlova, A. R. Junghans, B. Jurado, D. Karamanis, A. Kelić, R. Legrain, S. Leray, R. A. Mewaldt, B. Mustapha, M. F. Ordonez, J. Pereira, M. Pravikoff, F. Rejmund, M. V. Ricciardi, K.-H. Schmidt, C. Schmitt, C. Stéphan, K. Sümmerer, J. Taïeb, L. Tassan-Got, C. Villagrasa, F. Vivès, C. Volant, M. E. Wiedenbeck, W. Wlazole, N. E. Yanasak, and O. Yordanov.

References

- [1] R. Serber 1947 *Phys. Rev.* **72**, 1114.
- [2] J. Hüfner 1985 *Physics Reports* **125**, 129.

- [3] L.G. Moretto (1975) *Nucl. Phys. A* **247**, 211.
- [4] L.G. Moretto and G.J. Wozniak (1989) *Pramana, J. Phys.* **33**, 209.
- [5] L.G. Moretto and G.J. Wozniak (1993) *Ann. Rev. Nucl. Part. Sci.* **43**, 379.
- [6] G.C. Bonsignori et al (2001) Bologna 2000: Structure of the Nucleus at the Dawn of the Century, Vol. I: NucleusNucleus Collisions, Sections IIV, World Scientific, Singapore.
- [7] V.E. Viola, K. Kwiatkowski, L. Beaulieu, D.S. Bracken, H. Breuer, J. Brzychczyk, R.T. de Souza, D.S. Ginger, W-C. Hsi, R.G. Korteling, T. Lefort, W.G. Lynch, K.B. Morley, R. Legrain, L. Pienkowski, E.C. Pollacco, E. Renshaw, A. Ruangma, M.B. Tsang, C. Volant, G. Wang, S.J. Yennello and N.R. Yoder (2006) *Phys. Rep.* **434**, 1.
- [8] V.A. Karnaukhov, S.P. Avdeyev, E.V. Duginova, L.A. Petrov, V.K. Rodionov, H. Oeschler, A. Budzanowski, W. Karcz, M. Janicki, O.V. Bochkarev, E.A. Kuzmin, L.V. Chulkov, E. Norbeck and A.S. Botvina (2003) *Yad. Fiz.* **66**, 1282; (2003) *Phys. Atomic Nuclei* **66**, 1242.
- [9] G.F. Bertsch and P.J. Siemens (1983) *Phys. Lett. B* **126**, 9.
- [10] P.J. Siemens (1983) *Nature* **305**, 410.
- [11] J. Richert and P. Wagner (2001) *Phys. Reports C* **350**, 1.
- [12] A. Bonasera, M. Bruno, C.O. Dorso and P.F. Mastinu (2000) *Rev. Nuovo Cim.* **23**, 1.
- [13] Ph. Chomaz, M. Colonnab and J. Randrup (2004) *Phys. Rep.* **389**, 263.
- [14] W.A. Friedman and W.G. Lynch (1983) *Phys. Rev. C* **28**, 16.
- [15] J.A. López and J. Randrup (1989) *Nucl. Phys. A* **503** , 183.
- [16] R.J. Charity, M.A. McMahan, G.J. Wozniak, R.J. McDonald, L.G. Moretto, D.G. Sarantites, L.G. Sobotka, G. Guarino, A. Pantaleo, L. Fiore, A. Gobbi and K.D. Hildenbrand (1988) *Nucl. Phys. A* **483**, 371.
- [17] J. Randrup and S.E. Koonin (1981) *Nucl. Phys. A* **356**, 223.
- [18] G. Fai and J. Randrup (1982) *Nucl. Phys. A* **381**, 557.
- [19] J. Randrup (1993) *Comp. Phys. Comm.* **77**, 153.
- [20] A.S. Botvina, A.S. Iljinov and I.N. Mishustin (1985) *Yad. Fiz.* **42**, 1127; (1985) *Sov. J. Nucl. Phys.* **42**, 712.
- [21] J.P. Bondorf, R. Donangelo, I.N. Mishustin and H. Schulz (1985) *Nucl. Phys. A* **444**, 460.
- [22] J.P. Bondorf, A.S. Botvina, A.S. Iljinov, I.N. Mishustin and K. Sneppen (1995) *Phys. Rep.* **257**, 133.

- [23] D.H.E. Gross (1990) *Rep. Prog. Phys.* **53**, 605.
- [24] D.H.E. Gross (1997) *Phys. Rep.* **279**, 119.
- [25] H. Geissel, P. Armbruster, K.H. Behr, A. Brünle, K. Burkard, M. Chen, H. Folger, B. Franczak, H. Keller, O. Klepper, B. Langenbeck, F. Nickel, E. Pfeng, M. Pfützner, E. Roeckl, K. Rykaczewski, I. Schall, D. Schardt, C. Scheidenberger, K.-H. Schmidt, A. Schroter, T. Schwab, K. Sümmerer, M. Weber, G. Münzenberg, T. Brohm, H.-G. Clerc, M. Fauerbach, J.-J. Gaimard, A. Grewe, E. Hanelt, B. Knödler, M. Steiner, B. Voss, J. Weckenmann, C. Ziegler, A. Magel, H. Wollnik, J.P. Dufour, Y. Fujita, D.J. Vieira and B. Sherrill (1992) *Nucl. Instrum. Methods B* **70**, 286.
- [26] K.-H. Schmidt, E. Hanelt, H. Geissel, G. Mnzenberg and J.-P. Dufour (1987) *Nucl. Instr. Methods A* **260**, 287.
- [27] P. Armbruster, J. Benlliure, M. Bernas, A. Boudard, E. Casarejos, S. Czajkowski, T. Enqvist, S. Leray, P. Napolitani, J. Pereira, F. Rejmund, M.-V. Ricciardi, K.-H. Schmidt, C. Stéphan, J. Taieb, L. Tassan-Got and C. Volant (2004) *Phys. Rev. Lett.* **93**, 212701.
- [28] J. Taieb, K.-H. Schmidt, L. Tassan-Got, P. Armbruster, J. Benlliure, M. Bernas, A. Boudard, E. Casarejos, S. Czajkowski, T. Enqvist, R. Legrain, S. Leray, B. Mustapha, M. Pravikoff, F. Rejmund, C. Stéphan, C. Volant and W. Wlazlo (2003) *Nucl. Phys. A* **724**, 413.
- [29] J.P. Dufour, H. Delagrange, R. Del Moral, A. Fleury, F. Hubert, Y. Llabador, M.B. Mauhourat, K.-H. Schmidt and A. Lleres (1982) *Nucl. Phys. A* **387**, 157c.
- [30] R.J. Charity (1998) *Phys. Rev.* **58**, 1073.
- [31] M. Bernas, P. Armbruster, J. Benlliure, A. Boudard, E. Casarejos, S. Czajkowski, T. Enqvist, R. Legrain, S. Leray, B. Mustapha, P. Napolitani, J. Pereira-Conca, F. Rejmund, M.V. Ricciardi, K.-H. Schmidt, C. Stéphan, J. Taieb, L. Tassan-Got and C. Volant (2003) *Nucl. Phys. A* **725**, 213.
- [32] M. V. Ricciardi, P. Armbruster, J. Benlliure, M. Bernas, A. Boudard, S. Czajkowski, T. Enqvist, A. Kelic, S. Leray, R. Legrain, B. Mustapha, J. Pereira, F. Rejmund, K. -H. Schmidt, C. Stéphan, L. Tassan-Got, C. Volant and O. Yordanov (2006) *Phys. Rev. C* **73**, 014607.
- [33] M. V. Ricciardi, P. Armbruster, J. Benlliure, M. Bernas, A. Boudard, S. Czajkowski, T. Enqvist, A. Kelic, S. Leray, R. Legrain, B. Mustapha, J. Pereira, F. Rejmund, K. -H. Schmidt, C. Stéphan, L. Tassan-Got, C. Volant and O. Yordanov (2006) *Phys. Rev. C* **73**, 014607.
- [34] T. Enqvist, W. Wlazlo, P. Armbruster, J. Benlliure, M. Bernas, A. Boudard, S. Czajkowski, R. Legrain, S. Leray, B. Mustapha, M. Pravikoff, F. Rejmund, K.-H. Schmidt, C. Stéphan, J. Taieb, L. Tassan-Got and C. Volant (2001) *Nucl. Phys. A* **686**, 481.

- [35] A. Kelic, K.-H. Schmidt, T. Enqvist, A. Boudard, P. Armbruster, J. Benlliure, M. Bernas, S. Czajkowski, R. Legrain, S. Leray, B. Mustapha, M. Pravikoff, F. Rejmund, C. Stéphan, J. Taieb, L. Tassan-Got, C. Volant and W. Wlazlo (2004) *Phys. Rev. C* **70**, 064608.
- [36] C. Villagrasa et al., In preparation.
- [37] P. Napolitani, K.-H. Schmidt, A.S. Botvina, F. Rejmund, L. Tassan-Got and C.Villagrasa *Phys. Rev. C* **70**, 054607 (2004).
- [38] U.L. Businaro and S. Gallone (1955) *Nuovo Cimento* **1**, 629.
- [39] U.L. Businaro and S. Gallone (1955) *Nuovo Cimento* **1**, 1277.
- [40] P. Napolitani, K.-H. Schmidt, L. Tassan-Got et al. in preparation.
- [41] D. Henzlova (2005) *PHD thesis: Systematic investigation of the isotopic distributions measured in the fragmentation of ^{124}Xe and ^{136}Xe projectiles*, GSI, Darmstadt (Germany).
- [42] M. Pichon, B. Tamain, R. Bougault, F. Gulminelli, O. Lopez, E. Bonnet, B. Borderie, A. Chbihi, R. Dayras, J.D. Frankland, E. Galichet, D. Guinet, P. Lantesse, N. Le Neindre, M. Pârlog, M.F. Rivet, R. Roy, E. Rosato, E. Vient, M. Vigilante, C. Volant, J.P. Wieleczko and B. Zwieglinsk (2006) *Nucl. Phys. A* in press.
- [43] R. Bass, *Proceedings: Symposium on Deep-Inelastic and Fusion Reactions with Heavy Ions, Berlin 1979*, Springer-Verlag, Berlin 1979.
- [44] R. Bass, *Nuclear Reactions with Heavy Ions*, Springer-Verlag, Berlin 1980.
- [45] B.D. Wilkins, E.P. Steinberg and R.R.Chasman (1976) *Phys. Rev. C* **14**, 1832.
- [46] Böckstiegel, S.Steinhäuser, J.Benlliure, H.-G. Clerc, A. Grewe, A. Heinz, M. de Jong, A.R. Junghans, J. Müller and K.-H. Schmidt (1997) *Phys. Lett. B* **398**, 259.
- [47] O.A.P. Tavares and M.L. Terranova (1992) *Nuovo Cim. A* **105**, 723.